Mimicking mussel adhesion to improve interfacial properties in composites

L. M. Hamming[1], **X. W. Fan**[2], **P. B. Messersmith**[1,2], and **L. C. Brinson**[1,3]

[1] Materials Science and Engineering Department, Northwestern University, 2145 Sheridan Rd., Evanston, IL 60208

[2] Biomedical Engineering Department, Northwestern University, 2145 Sheridan Rd., Evanston, IL 60208

[3] Mechanical Engineering Department, Northwestern University, 2145 Sheridan Rd., Evanston, IL 60208

Abstract

The macroscale properties of polymer-matrix composites depend immensely on the quality of the interaction between the reinforcement phase and the bulk polymer. This work presents a method to improve the interfacial adhesion between metal-oxides and a polymer matrix by performing surface-initiated polymerization (SIP) by way of a biomimetic initiator. The initiator was modeled after 3,4-dihydroxy-L-phenylalanine (dopa), an amino acid that is highly concentrated in mussel foot adhesive proteins. Mechanical pull out tests of NiTi and Ti-6Al-4V wires from poly (methyl methacrylate) (PMMA) were performed to directly test the interfacial adhesion. These tests demonstrated improvements in maximum interfacial shear stress of 116% for SIP-modified NiTi wires and 60% for SIP-modified Ti-6Al-4V wires over unmodified specimens. Polymer chain growth from the metal oxides was validated using x-ray photoemission spectroscopy (XPS), ellipsometry, scanning electron microscopy (SEM), and contact angle analysis.

Keywords

A. Polymer-matrix composites (PMCs); B. Fiber/matrix bond; B. Interfacial strength; B. Surface treatments; B. Interphase

L. C. Brinson
Northwestern University, Robert R McCormick School Engineering & Applied Science, Department of Materials Science & Engineering, 2145 Sheridan Rd., Evanston, IL 60208 USA
Northwestern University, Robert R McCormick School Engineering & Applied Science, Department of Mechanical Engineering, 2145 Sheridan Rd., Evanston, IL 60208 USA
E-mail Address: cbrinson@northwestern.edu
Phone: 847-467-2347
Fax: 847-263-0540
P. B. Messersmith
Northwestern University, Robert R McCormick School Engineering & Applied Science, Department of Biomedical Engineering, 2145 Sheridan Rd, Evanston, IL 60208 USA
Northwestern University, Robert R McCormick School Engineering & Applied Science, Department of Materials Science & Engineering, 2145 Sheridan Rd, Evanston, IL 60208 USA
E-mail Address: philm@northwestern.edu
Phone: 847-467-5273
Fax: 847-491-4928

1. Introduction

In this paper, we aim to demonstrate a dramatic improvement in adhesion between a metal-oxide and a surrounding polymer by performing surface-initiated polymerization (SIP) using a biomimetic initiator. While the properties of a composite depend on the properties of the constituents (for example carbon fibers and epoxy), the quality of the interaction between the phases critically determines performance [1,2]. Strong interfaces are necessary for efficient load transfer to the reinforcement phase to increase the stiffness of the composite [2–4]. For improved toughness, the interfacial adhesion should be high but still allow for some energy dissipation through debonding [5]. Therefore, optimizing the interfacial properties between different phases is an important factor in designing composites with maximum load transfer and increased strength and toughness.

There are a host of reinforcing materials, such as metals, silica, and carbon nanotubes that could be utilized to increase the strength and stiffness of a polymer. One especially interesting possibility for reinforcement is NiTi due to its unique properties: the shape memory effect (SME) and pseudoelasticity (PE) [3]. These effects result from a diffusionless phase transformation between an austenitic and martensitic crystallographic structure in response to heating and cooling or mechanical deformation. When starting in the martensitic regime, shape memory alloys (SMA) can be deformed but then return to their original shape after heating induces an austenite phase transformation. If originally in the austenitic regime, PE materials can be strained up to 8% and fully recover their original shape upon unloading [6]. These recoverable deformations are far beyond a typical metal's yield point of 0.02%. Researchers hope to capitalize on these properties to create smart materials such as thermo-mechanical actuators [3,7–9], self-healing composites [10], and impact and creep resistance structures [11]. In such applications of SMA composites, maximum interfacial adhesion is necessary to effectively transfer the load from the matrix to the filler.

It is especially important to optimize the interfacial properties in nanocomposites as the reinforcing phase has an extremely high surface area to volume ratio [12]. In nanocomposites, an interphase zone with structure and properties different than those of the bulk polymer naturally surrounds each nano-sized particle [13,14]. The ultimate goal of modifying the surface of the nano-sized particles is to improve the particle-matrix coupling characteristics of the interphase zone while simultaneously preventing particle-particle aggregation [15]. If these two objectives are satisfied, the properties of the entire composite can be transformed with small additions of nano-sized particles.

One of the simplest methods to increase interfacial adhesion in composites is to increase the surface roughness of the reinforcement phase by sandblasting [3]. The increased roughness will lead to mechanical interlocking during pull out. While this method is simple to perform on large reinforcements, it cannot be performed when the reinforcement phase is on the same size-scale or smaller than grains of sand. Another method to increase the interfacial adhesion between metal oxides and polymers is through the use of silane coupling agents. Silane coupling agents have one Si group that interacts with various inorganic surfaces and another group that reacts with organic materials. This strategy is widely used in dental composites to increase the interaction between the reinforcement phase and the polymer host [16]. However, researchers have found that the stability of silane coupling agents (Ti-O-Si and Zr-O-Si) in aqueous environments is low [17]. Consequently, if metal-oxides are to be used as reinforcements in biomedical or structural applications where water is present, there is a need for interfacial adhesions that remain robust in aqueous environments allowing for proper stress transfer and longer-lasting mechanical integrity.

For the purpose of creating a surface modification technique that is stable in aqueous environments, we approached interfacial design from a biomimetic perspective. By incorporating chemical constituents found in adhesive proteins secreted by mussels, we designed an initiator for surface initiated polymerization [18] and demonstrated its use on TiO_2 nanoparticles [19].

Marine mussels, like *Mytilus edulis*, use a natural adhesive to adhere to virtually any surface even in the presence of waves and tides [20,21]. Researchers have been unable to synthesize an adhesive as strong, versatile, and unaffected by water as the mussel's glue. The unusual amino acid dopa makes up 20 mol% of the *Mytilus edulis* foot protein-3 [22] and 26 mol% of foot protein-5 [23] that are found at the substrate-pad interface. A single dopa molecule was found to bind reversibly to TiO_2 surfaces with a dissociation force of 805 pN in the presence of water [24]. To put 805 pN in perspective, single molecule atomic force microscopy (AFM) experiments revealed a dissociation force of 2000 pN for the silicon-carbon covalent bond [25] and approximately 10–20 pN for the unzipping of DNA hydrogen bond pairs [26]. Therefore, the dopa-titania interaction of 805 pN is quite strong and robust in aqueous environments making it an attractive candidate to emulate in efforts to improve the adhesion in inorganic-polymer composites.

In this paper, we demonstrate that our dopa-initiator is as effective as silane coupling agents in improving interfacial adhesion in inorganic- polymer composites. We grafted PMMA polymer coatings from NiTi and Ti-6Al-4V wires by SIP using our dopa-mimetic initiator. As TiO_2 is found abundantly on NiTi oxide surfaces, dopa should also bind well to NiTi substrates [27]. We then quantified the improvement in interfacial adhesive properties between the SIP-modified alloy wires and polymer systems by performing single fiber pull out experiments of the wires embedded in a PMMA matrix. By pulling out a fiber embedded in another material, one can quantify the interfacial properties of the system by examining the relationship between peak load and embedded length. In short fiber or nanoreinforced composites, every particle intersecting a fracture plane is essentially subjected to a fiber pull out test during fracture. Macroscale fiber pull out tests offer an indication of this reinforcement behavior. At the nanoscale, the surface modification should have an even more dramatic effect on the interfacial properties due to the larger surface area to volume ratio. Therefore, a measure of the improvement in interfacial adhesion from our fiber pull out tests not only characterizes the adhesive behavior of macroscale composites, but also has implications for the reinforcement-ability of TiO_2-containing nanoparticles in polymer nanocomposites.

2. Experimental

2.1 Materials

NiTi (55% Ni, 45% Ti) and Ti-6Al-4V (Grade 5, alloy of 6% aluminum and 4% vanadium, extra low interstitials) wires with a diameter of 0.127 mm were purchased from Small Parts, Inc. (Miami Lakes, Florida). For flat, reference substrates, silicon wafers were coated with a 20 nm-thick layer of TiO_2 (99.9% pure, West Cerac, Milwaukee, WI) by electron beam evaporation (Edwards Auto306; <10-5 Torr). The coated wafers were diced into 1 cm by 1 cm pieces for use in contact angle analysis, ellipsometry, and XPS. Ultrapure water (resistivity = 18.2 MΩ, pH 6.82) was obtained from a NANOpure Infinity system from Barnstead/Thermolyne Corporation (Dubuque, Iowa). MMA monomer (99%, Aldrich, St. Louis, MO) was passed through an activated alumina gel column to remove inhibitor before polymerization. Other materials used as received include Copper (I) bromide (CuBr, 99.999%, Aldrich, St. Louis, MO), 4,8,11-tetraazacyclotetradecane (Me$_4$cyclam, Aldrich, St. Louis, MO), dimethylformamide (DMF, Sigma, St. Louis, MO), 2-propanol (Aldrich, St. Louis, MO), acetone (VWR International, West Chester, PA), and petroleum ether (Sigma-

Aldrich, St. Louis, MO). Poly(methyl methacrylate) (PMMA) of MW 75,000 was purchased from Polysciences, Inc. (Warrington, PA). The dopa-mimetic initiator was synthesized as previously described [18].

2.2 Preparation of SIP-modified inorganic wires

NiTi and Ti-6Al-4V wires were cut into 30 mm lengths and ultrasonically cleaned for 10 minutes in acetone, ultrapure water (UP), petroleum ether, and then 2-propanol. After drying, the metal wires were further cleaned with oxygen plasma for 3 minutes. The wires were then submerged in a solution of 3 mg of the dopa-mimetic initiator in 3 mL UP water. The wires were soaked in darkness overnight to allow the initiator to bind to the wire surface and to prevent initiator oxidation. After 18 hours, the wires were rinsed in UP water to remove unbound initiator and then dried with N_2.

In one flask, 4.38 mL DMF, 1.62 mL UP water, and 6 mL MMA monomer were stirred and purged under Ar for 20 minutes. 36 mg Me_4cyclam and 20.4 mg CuBr were then added to the solution and a blue color change was observed. The inorganic wires with immobilized initiator were placed in a second flask set in an oil bath at 60°C. Both flasks were purged under Ar for an additional hour. Once all solids were completely dissolved and a homogeneous blue solution was obtained in the first flask, the solution was transferred with a degassed syringe into the second flask containing the inorganic wires. The solution remained under Ar and 60°C for 20 hours during surface initiated atom transfer radical polymerization (ATRP). The SIP-modified wires were then rinsed with DMF and acetone to remove any unbound species.

2.3 Instrumentation

Reference samples and wires were cleaned in a plasma chamber from Harrick Scientific (Ossining, New York). Grafted PMMA thicknesses on flat reference samples were measured by an ESM-300 ellipsometer from J. A. Woollam, Inc. (Lincoln, NE). XPS analysis was performed on an ESCALAB system from Omicron (Taunusstein, Germany) to determine the surface composition of both unmodified and modified metal oxide surfaces. Contact angle measurements were performed on a custom-built instrument with components from Rame-Hart, Inc. (Netcong, NJ). Qualitative analysis of the wires during each experimental stage was carried out on a LEO Gemini 1525 SEM (Oberkochen, Germany). All wires were coated with 3 nm Au-Pd before imaging to reduce charging of the polymer. Wires were hot pressed in PMMA in a Carver Auto Series press (Wabash, IN). Wire pull out tests were performed in a MiniMat2000 miniature tensile tester from Rheometric Scientific (Piscataway, NJ).

2.4 Wire pull out setup

Figure 1 shows a schematic of the experimental procedure from wire preparation to wire pull out. A tensile pull out test was used to quantify the effect of our SIP-modification on interfacial adhesion between the wires and the polymer. The pull out setup was modeled after work done by Cordes and Daniel in which 0.1375 mm diameter SiC fibers were hot pressed between two barium borosilicate glass sheets for subsequent single fiber pull out tests [28]. In our experiment, SIP-modified wires and unmodified wires were hot pressed at 3.5 MPa and 200°C for 10 minutes between two 0.25 mm thick sheets of PMMA. The wires were sandwiched between the sheets so that approximately 15 mm of wire length was embedded while the other 15 mm protruded from the PMMA. Sand paper was glued with cyanoacrylate to both the free wire end as well as just below the embedded end to aid in clamping the specimen in the Minimat2000. Each end of the sample was clamped and loaded in tension at a rate of 0.5 mm/min. Between 9 and 16 pull out tests were performed on each type of specimen.

3. Results and Discussion

3.1 Characterization of SIP-modification on wires

To verify that we successfully performed ATRP from our metal-oxide wires, flat NiTi and Ti-6Al-4V reference substrates were included with the wires during synthesis and used for thickness, contact angle measurements, and chemical analysis. Ellipsometry on the SIP-modified flat reference surfaces revealed a PMMA grafted thickness of 93 ± 4 nm on the NiTi and 120 ± 5 nm on the Ti-6Al-4V. The static water contact angle increased from $10°$ after solvent cleaning and oxygen plasma etching on the unmodified metals to $82°$ for SIP-modified NiTi and $70°$ for SIP-modified Ti-6Al-4V substrates. The increase in static water contact angle is consistent with the grafting of hydrophobic PMMA chains from the metal substrates during SIP. Imparting a hydrophobicity on surfaces may decrease the aggregation in future applications by increasing the compatibility of nanoparticles in hydrophobic polymers [29].

Figure 2 shows XPS spectra for the unmodified and SIP-modified NiTi reference surfaces. In Figure 2a, the Ti2p peak is associated with the TiO_2 species found at the surface of unmodified NiTi [27]. The complete disappearance of the Ti2p peak and detection of only C and O in Figure 2b confirms full coverage of the NiTi surface with the PMMA brushes after ATRP. XPS chemical composition on the modified sample indicates a composition of 24.2% oxygen and 75.8% carbon, similar to the theoretical composition of 28.6% oxygen and 71.4% carbon for PMMA. XPS showed similar results for the Ti-6Al-4V reference sheet. Ellipsometry, contact angle analysis and XPS indicate successful grafting of PMMA chains from the NiTi and Ti-6Al-4V surfaces.

Figure 3 shows SEM images during progressive steps of preparation of SIP-modified inorganic wires and wire pull outs described in the experimental section. Figure 3a is an image of a cleaned, unmodified Ti-6Al-4V wire. Figure 3b shows the immobilized initiator on the wire surface. Figure 3c is an image taken after 20 hours of ATRP from the initiator and metal surface. Notice that the surface in Figure 3c is smoother than in 3a indicating full coverage of the metal with PMMA chains. Finally, Figure 3d is an image of the surface of the wire after pull out. Again the surface is smoother than in Figure 3a indicating PMMA is retained on the Ti-6Al-4V surface after pull out.

Representative mages of an unmodified Ti-6Al-4V wire after pull out and a SIP-modified Ti-6Al-4V wire after pull out from bulk PMMA are shown in Figures 4a and 4b, respectively. The diameter of the unmodified wire after pull out is 125.6 μm (close to the manufacturer's listing of 127 μm) while the largest diameter for the SIP-modified wire after pull out is 172.5 μm. The marked difference in debris attached to the two wires indicates a stronger interaction with the bulk polymer for the modified wire than the unmodified wire. We hypothesize that anchoring by the strong catechol-titanium interaction in our system as well as entangling of the grafted polymer chains with the bulk polymer led to a higher force required for pull out and more residual polymer compared to the unmodified wire.

3.2 Force versus displacement curves from wire pull out tests

Figures 5a and 5b show representative force versus displacement curves for the SIP-modified and the unmodified wires pulled out from PMMA. As the wire is pulled, a crack was observed to propagate down the length of the wire gradually debonding it from the polymer matrix. The point of complete debonding is marked with an asterisk in the figures. After the asterisk, there is a sharp drop in force indicating the wire is no longer adhered to the polymer.

The multiple, jagged peak features of the SIP-modified sample in Figure 5a are due to progressive stress-induced martensitic phase transformations that occur down the length of the pseudoelastic shape memory alloy wires. When strained, pseudoelastic materials undergo a martensitic phase transformation from a parent austenitic phase resulting in up to 8% inelastic strains that are spontaneously recovered upon unloading [30]. To confirm the austenite to martensite diffusionless phase transformation, a stress-strain tensile test was performed on a bare NiTi wire (not embedded in PMMA). The NiTi wire was loaded to 4.3% strain at a rate of 0.5 mm/min and subsequently unloaded. The threshold peak in Figure 6 arises because it takes more energy to initiate the austenite to martensite transformation than to propagate the transformation. The complete, closed hysteresis loop in Figure 6 indicates that the wire recovered its original shape after unloading. Therefore, the wire is in the austenitic state at room temperature, transforms to a martensitic phase above a threshold force (~8.5 N or 660 MPa), and then returns to the austenitic phase upon unloading.

The transformation force (~8.5 N or 660 MPa) in Figure 6 corresponds well with the first peak value of 8.71 N in the pull out curve of Figure 5a and is similar to the mean transformation value of 9.1 N for all 16 modified NiTi cases. The similarity in values supports our notion that the jagged features represent an austenite to martensite phase transformation. We suggest that the multiple jagged features represent a series of segments debonding then transforming down the length of the wire during pull-out. In contrast, the untreated NiTi wires do not show such multiple peaks because total wire-polymer interface failure occurs before the onset of the austenite to martensite phase transformation at approximately 8.5 N. As expected, Ti-6Al-4V wires in Figure 4b exhibit only a single peak during debonding because Ti-6Al-4V does not exhibit PE behavior as in the case of NiTi.

In both Figures 5a and 5b, the modified wires reach a maximum force significantly greater than that of the unmodified metal wires. Taking into account the variations in embedded length from sample to sample, we calculated a simple maximum interfacial shear stress, τ_m, required for complete debonding as:

$$\tau_m = \frac{F_m}{2\pi r l}$$

where F_m is the maximum force reached before complete debonding, r is the wire radius, and l is the embedded length. Figure 7 displays the average τ_m calculated for each type of sample. Our SIP-modified NiTi wires demonstrated an increase in maximum interfacial shear strength of 116% over the unmodified NiTi wires and our SIP-modified Ti-6Al-4V wires showed an improvement of 60% in maximum interfacial shear stress before debonding. Student's t-tests indicate the probability of obtaining each of these results, assuming the null hypothesis, is less than 0.00013.

3.3 Discussion

Several researchers have investigated methods of improving the reinforcement capabilities of inorganic constituents [1,3,5,31] in organic matrices for composite applications. At the macro-scale, increasing the surface roughness of the samples increases interfacial adhesion due to mechanical interlocking [1]. Jonnalagadda, Kline, and Sottos varied the surface treatments of SMA NiTi wires with diameter of 150 μm and then performed pull out tests to compare the resulting adhesive properties to epoxy matrices [3]. The researchers found that sandblasting the wires resulted in a 190% improvement in debond stress over untreated wires during pull out. With photoelastic stress analysis, they further demonstrated a 62%

increase in stress induced within the matrix during shape memory activation for the sandblasted wires over the untreated wires. These results reiterate the importance of high interfacial adhesion between constituents for optimal stress transfer in many SMA composite applications.

However, sand blasting is a destructive process and as the size of the reinforcing constituents moves to smaller scales, the method becomes impossible because the grains of sand become larger than the material of interest. Therefore, size-scale independent methods for improving interfacial adhesion are necessary. Toward this end, Smith et al. functionalized NiTi wires with silane coupling agents to link a metal-oxide surface to a chemical species that can be integrated into the polymerization of the matrix [31]. Silane coupling agents offer a size-scale independent method commonly utilized in dental composites to improve interfacial adhesion between fillers and matrix [16,31]. The researchers varied the coupling agent (APTS, MPS), the initiator (BPO, BPO/Benzoin, or AIBN), and curing conditions (thermal or UV). The silane coupling agents were chosen to react with metal-oxides on one end through a Si-Cl or Si-methoxy bond and have similar structures to PMMA monomer on the other end. From single fiber pull out tests, they found an increase in maximum adhesion strength for the APTS/AIBN UV cured samples of 114% and an increase in APTS/AIBN thermally cured samples of 91% over the unfunctionalized wires [31].

These values are comparable to the 116% increase in maximum interfacial shear stress we found for NiTi wires in PMMA, however other researchers have discovered that silane coupling agents are not stable in aqueous environments [17]. Trifunctional silanes have better hydrolytic stability than monofunctional silanes, but this is attributed to horizontal bonding rather than direct bonding to TiO_2 [17]. Further demonstrating this point, the systems initiated with BPO in Smith et al.'s experiments resulted in smaller increases in maximum adhesion strength than the use of AIBN. The researchers believed the weaker performance resulted from the large amount of water in BPO which would prevent the silane coupling agent from adhering to the metal-oxide [31].

To overcome this problem, we created a method for surface modification that is size-scale independent and should remain robust in aqueous environments as it is modeled after marine mussel adhesion. We demonstrated 116% and 60% increases in maximum interfacial interaction for NiTi and Ti6Al4V wires, respectively. These increases are comparable to those shown by Smith et al. and Jonnalagadda et al. without the disadvantages associated with silane coupling agents and sand blasting.

4. Conclusions

Improving the interface between inorganic reinforcements and an organic matrix is of paramount importance when designing new composites with properties superior to those of the individual phases. One of the biggest challenges in the composites field is in optimizing the interfacial interaction to yield proper stress transfer and ideal bulk properties. For smart materials, such as SMA NiTi-polymer actuators, maximum load transfer is desirable. For structural or biomedical applications, the adhesion must remain strong even with prolonged exposure to water. To create a strong and robust interface for such applications, we utilized a dopa-mimetic initiator inspired by mussel adhesive proteins to modify metal-oxide surfaces through ATRP. Mechanical pull out tests demonstrated an increase in maximum interfacial adhesion of 116% for modified NiTi wires and 60% for modified Ti-6Al-4V wires from a PMMA matrix. In addition to the improved coupling of the metal-oxides to the polymer, this versatile approach is size-scale independent and should remain robust in aqueous environments.

Acknowledgments

References

1. Neuking K, Abu-Zarifa A, Youcheu-Kemtchou S, Eggeler G. Polymer/NiTi-composites: Fundamental aspects, processing and properties. Adv Eng Mat. 2005; 7(11):1014–1023.

2. Pukanszky B. Interfaces and interphases in multicomponent materials: past, present, future. Euro Poly J. 2005; 41(4):645–662.

3. Jonnalagadda K, Kline G, Sottos N. Local displacements and load transfer in shape memory alloy composites. Exp Mech. 1997; 37(1):78–86.

4. Eitan A, Fisher FT, Andrews R, Brinson LC, Schandler LS. Reinforcement mechanisms in MWCNT-filled polycarbonate. Composites Science and Technology. 2006; 66(9):1162–1173.

5. Wetherhold RC, Bos J. Ductile reinforcements for enhancing fracture resistance in composite materials. Theo App Fract Mech. 2000; 33(2):83–91.

6. Gall K, Tyber J, Brice V, Frick CP, Maier HJ, Morgan N. Tensile deformation of NiTi wires. J Biomed Mat Res Part A. 2005; 75A(4):810–823.

7. Song GB, Kelly B, Agrawal BN, Lam PC, Srivatsan TS. Application of shape memory alloy wire actuator for precision position control of a composite beam. J Mat Sci Eng Perf. 2000; 9(3):330–333.

8. Song GB, Kelly B, Agrawal BN. Active position control of a shape memory alloy wire actuated composite beam. Sm Mat Struct. 2000; 9(5):711–716.

9. Shu SG, Lagoudas DC, Hughes D, Wen JT. Modeling of a flexible beam actuated by shape memory alloy wires. Sm Mat Struct. 1997; 6(3):265–277.

10. Burton DS, Gao X, Brinson LC. Finite element simulation of a self-healing shape memory alloy composite. Mech Mat. 2006; 38(5–6):525–537.

11. Wei ZG, Sandstrom R, Miyazaki S. Shape memory materials and hybrid composites for smart systems - Part II Shape-memory hybrid composites. J Mat Sci. 1998; 33(15):3763–3783.

12. Eitan A, Fisher FT, Andrews R, Brinson LC, Schandler LS. Reinforcement mechanisms in MWCNT-filled polycarbonate. Comp Sci Tech. 2006; 66(9):1162–1173.

13. Liu H, Brinson LC. A hybrid numerical-analytical method for modeling the viscoelastic properties of polymer nanocomposites. J App Mech- Trans ASME. 2006; 73(5)

14. Schadler LS, Brinson LC, Sawyer WG. Polymer nanocomposites: A small part of the story. JOM. 2007; 59(3):53–60.

15. Balazs AC, Emrick T, Russell TP. Nanoparticle polymer composites: Where two small worlds meet. Science. 2006; 314(5802):1107–1110. [PubMed: 17110567]

16. Soh MS, Sellinger A, Yap AUJ. Dental Nanocomposites. Curr Nanosci. 2006; 2(4):373–381.

17. Marcinko S, Fadeev AY. Hydrolytic stability of organic monolayers supported on TiO2 and ZrO2. Langmuir. 2004; 20(6):2270–2273. [PubMed: 15835682]

18. Fan X, Lin L, Dalsin J, Messersmith P. Biomimetic anchor for surface-initiated polymerization from metal substrates. JACS. 2005; 127(45):15843–15847.

19. Fan X, Lin L, Messersmith P. Surface-initiated polymerization from TiO2 nanoparticle surfaces through a biomimetic initiator: A new route toward polymer-matrix nanocomposites. Comp Sci Tech. 2006; 66(9):1198–1204.

20. Waite JH. Adhesion a la Moule. Int Comp Bio. 2002; 42(6):1172–1180.

21. Lin Q, Gourdon D, Sun C, Holten-Andersen N, Anderson TH, Waite JH, Israelachvili JN. Proceedings of the National Academy of Science. Adhesion mechanisms of the mussel foot proteins mfp-1 and mfp-3. PNAS. 2007; 104(10):3782–3786. [PubMed: 17360430]

22. Papov VV, Diamond TV, Biemann K, Waite JH. Hydroxyarginine-Containing Polyphenolic Proteins in the Adhesive Plaques of the Marine Mussel Mytilus-Edulis. J Bio Chem. 1995; 270(34):20183–20192. [PubMed: 7650037]

23. Waite JH, Qin XX. Polyphosphoprotein from the adhesive pads of Mytilus edulis. Biochemistry. 2001; 40(9):2887–2893. [PubMed: 11258900]

24. Lee H, Scherer NF, Messersmith PB. Single-molecule mechanics of mussel adhesion. PNAS. 2006; 103(35):12999–13003. [PubMed: 16920796]

25. Grandbois M, Beyer M, Rief M, Clausen-Schaumann H, Gaub HE. How strong is a covalent bond? Science. 1999; 283(5408):1727–1730. [PubMed: 10073936]

26. Rief M, Clausen-Schaumann H, Gaub HE. Sequence-dependent mechanics of single DNA molecules. Nat Struct Bio. 1999; 6(4):346–349. [PubMed: 10201403]

27. Shabalovskaya S, Anderegg J, Laab F, Thiel P, Rondelli G. Surface conditions of nitinol wires, tubing, and as-cast alloys. The effect of chemical etching, aging in boiling water, and heat treatment. J Biomed Mat Res Part B. 2003; 65B(1):193–203.

28. Cordes RD, Daniel IM. Determination of interfacial properties from observations of progressive fiber debonding and pullout. Comp Eng. 1995; 5(6):633–648.

29. Rong MZ, Zhang MQ, Ruan WH. Surface modification of nanoscale fillers for improving properties of polymer nanocomposites: a review. Mat Sci Tech. 2006; 22(7):787–796.

30. Es-Souni M, Es-Souni M, Fischer-Brandies H. Assessing the biocompatibility of NiTi shape memory alloys used for medical applications. Anal Bioanal Chem. 2005; 381:557–567. [PubMed: 15660223]

31. Smith N, Antoun G, Ellis A, Crone W. Improved adhesion between nickel-titanium shape memory alloy and a polymer matrix via silane coupling agents. Comp Part A, App Sci Manuf. 2004; 35(11):1307–1312.

a)

b)
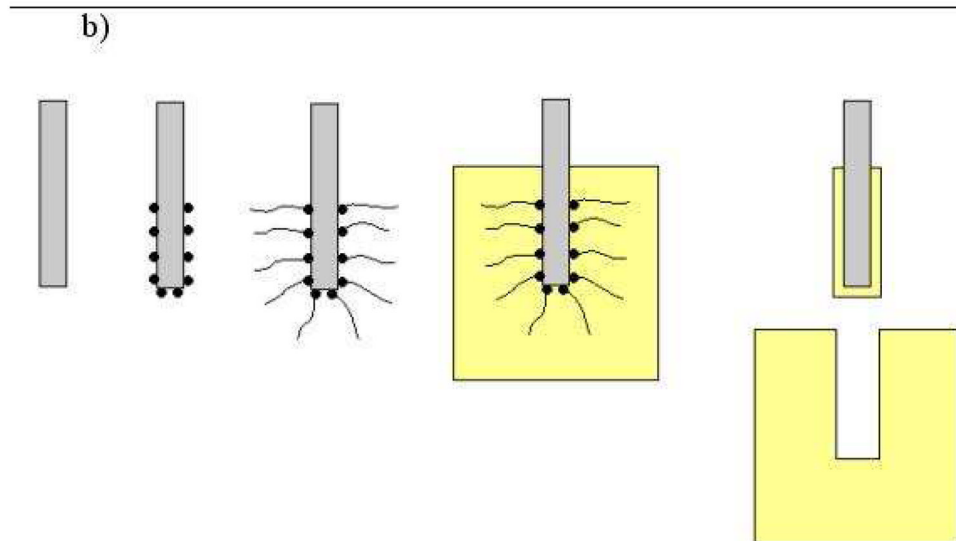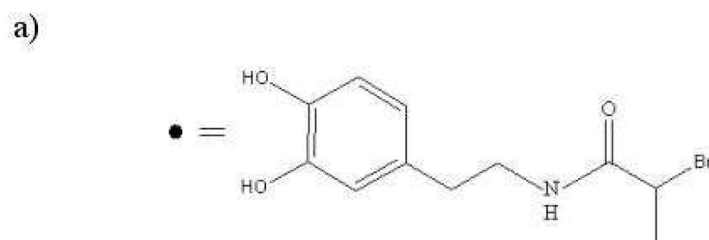
Figure 1.
a) Chemical structure of dopa-mimetic initiator. The catechol end of the initiator reacts strongly and reversibly with metal-oxide surfaces while the bromine terminus is available for SIP via atom transfer radical polymerization (ATRP). b) Schematic of the experimental steps including clean wires, immobilized initiator, SIP from initiator, wires embedded into PMMA matrix, and wires pulled out from bulk PMMA.
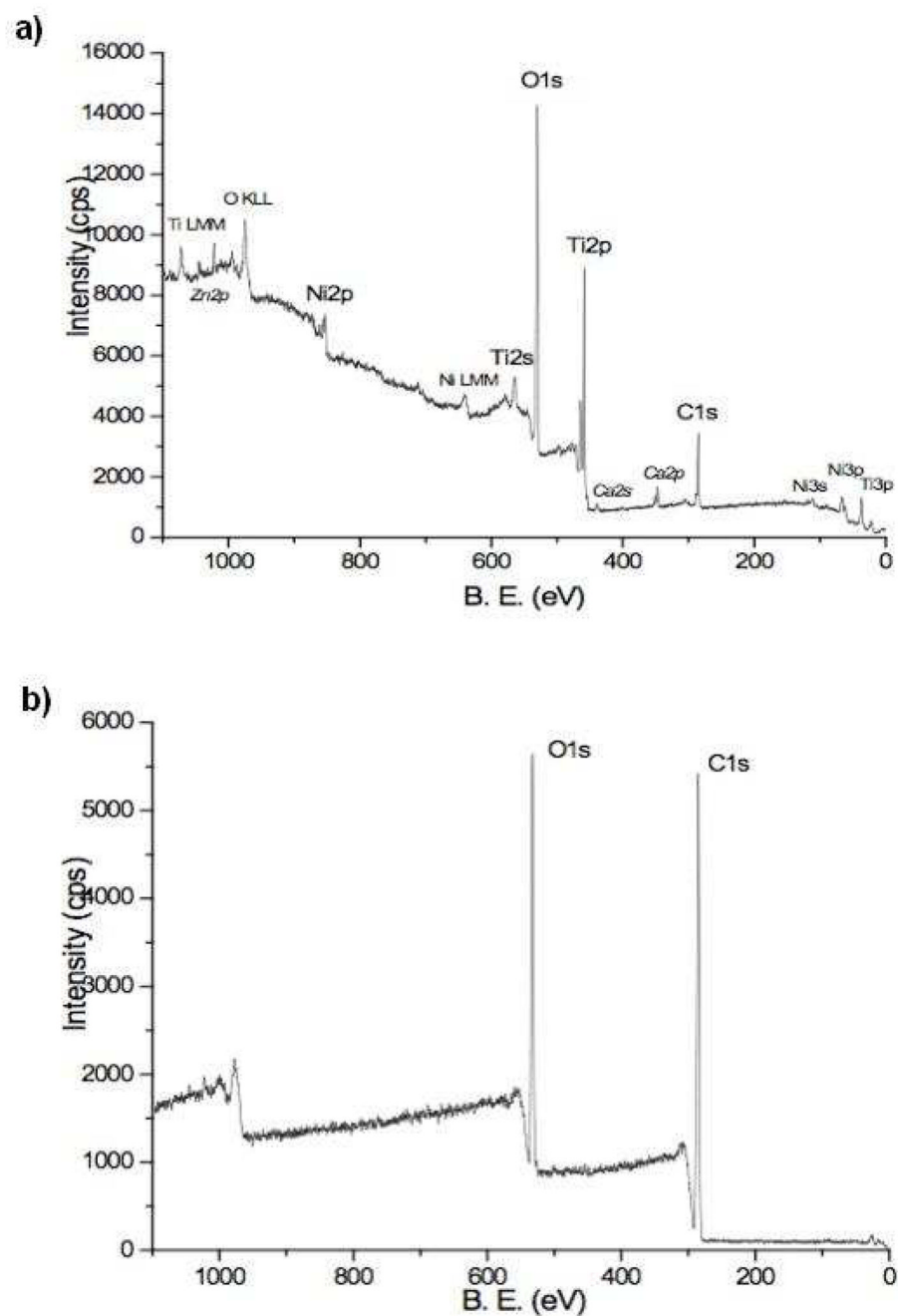
Figure 2.
a) XPS survey spectrum of a bare NiTi substrate. b) XPS survey spectrum of NiTi substrate after 20 hours of SI-ATRP. The Ti2p peak is notably absent indicating full coverage of the NiTi surface with grafted PMMA chains.
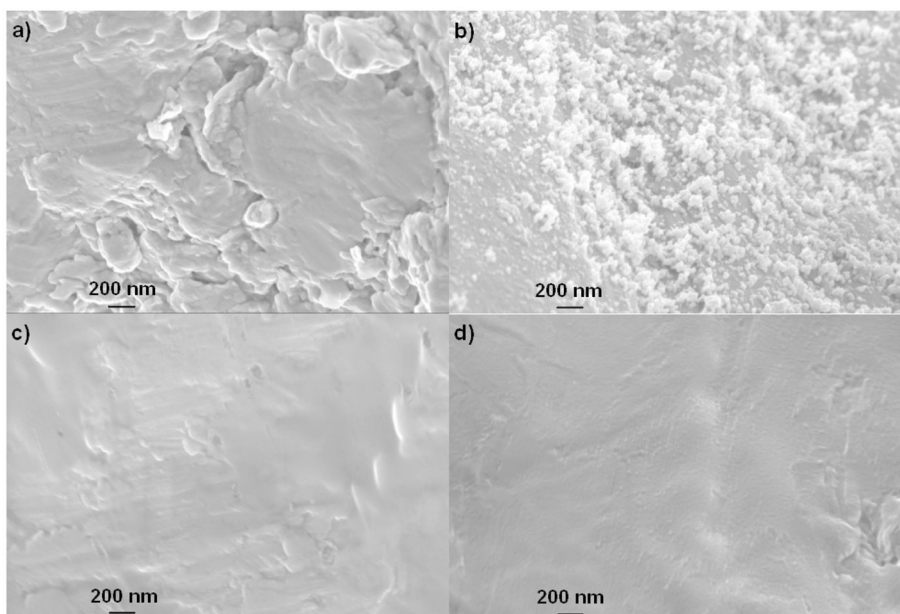
Figure 3.
SEM images of the surface structure of the Ti-6Al-4V wires of progressive experimental steps: a) clean wire, b) immobilized dopa-mimetic initiator, c) SIP from initiator, and d) wire pulled out from bulk PMMA.
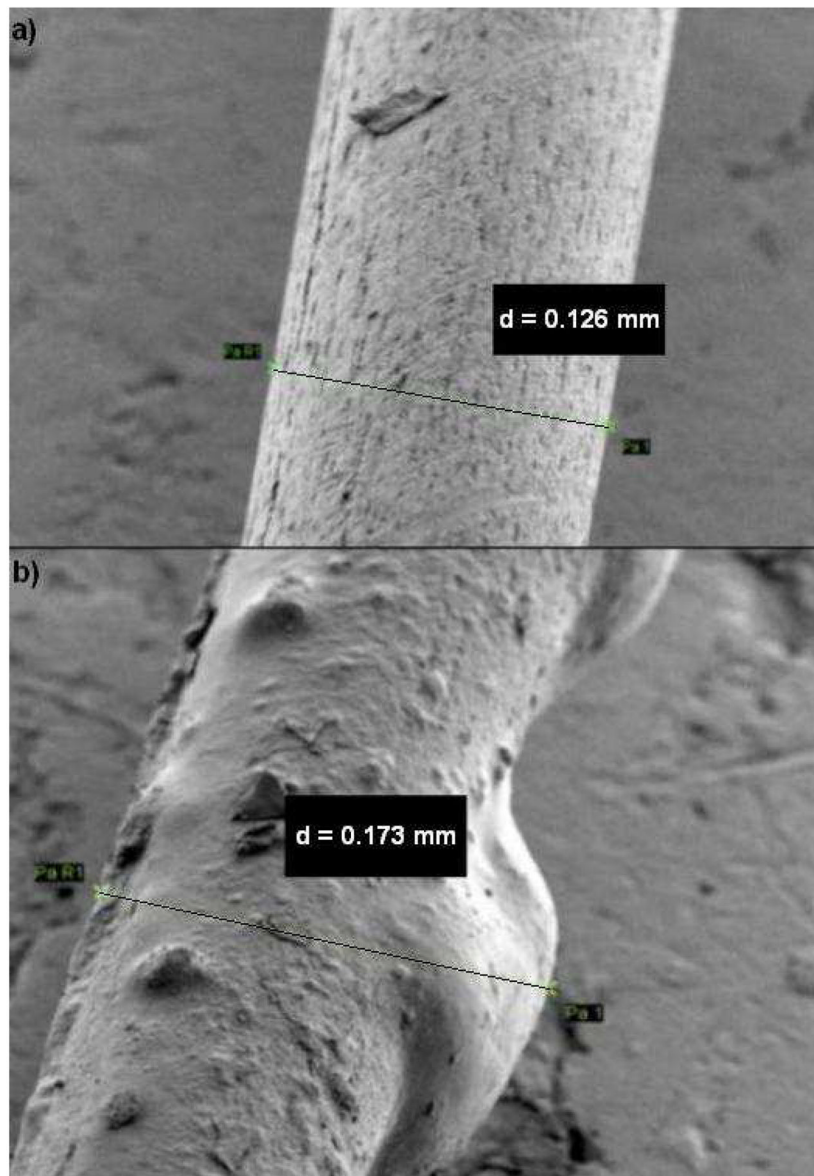
Figure 4.
a) Unmodified Ti-6Al-4V wire after pull out from bulk PMMA with a diameter of 125.6 μm. B) SIP-modified Ti-6Al-4V wire after pull out from bulk PMMA with a maximum diameter of 172.5 μm.
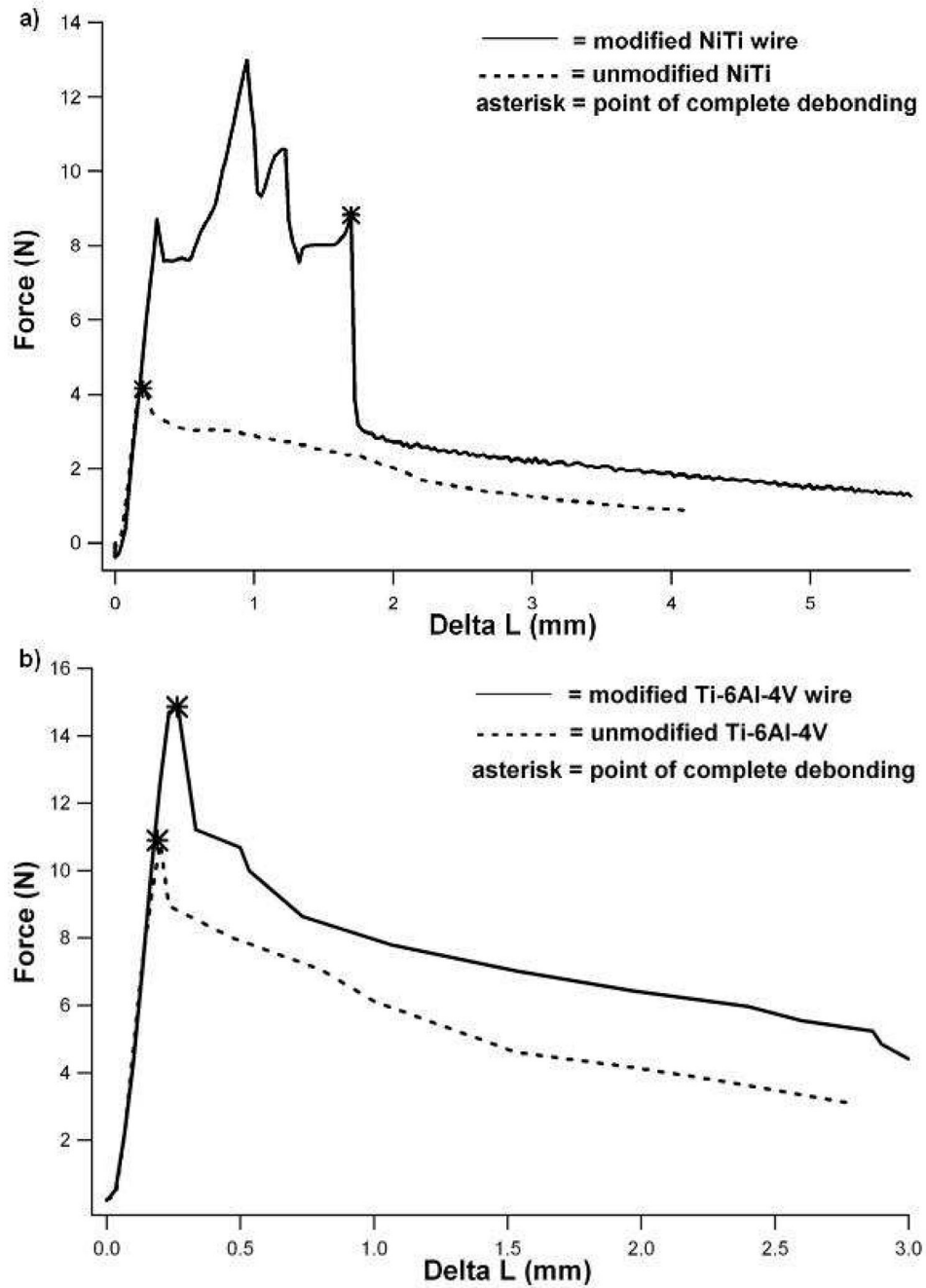
Figure 5.
a) Representative pull out curve for the SIP-modified and unmodified NiTi wires from PMMA. b) Representative pull out curve for the SIP-modified and unmodified Ti-6Al-4V wires from PMMA.
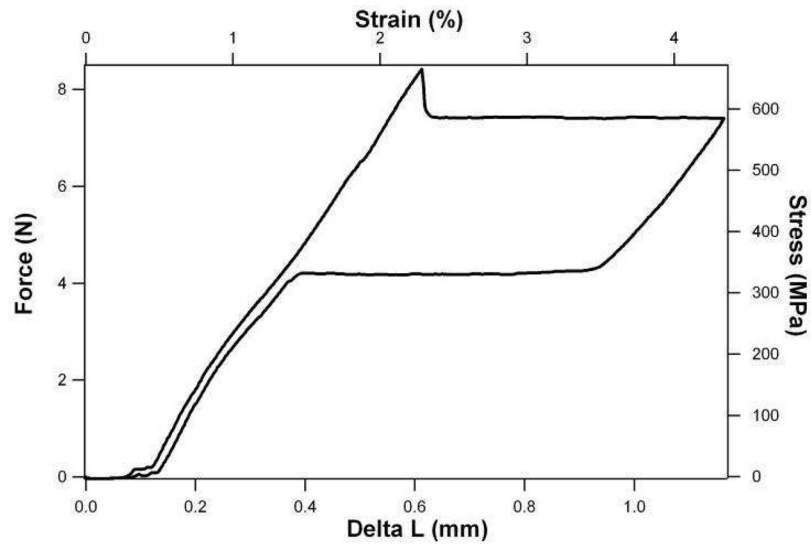
Figure 6.
Hysteresis curve for a pure NiTi wire specimen loaded to 4.3% strain then fully unloaded. The austenite to martensite transformation peak occurs at approximately 660 MPa (force of 8.5 N) and 2.3% strain.
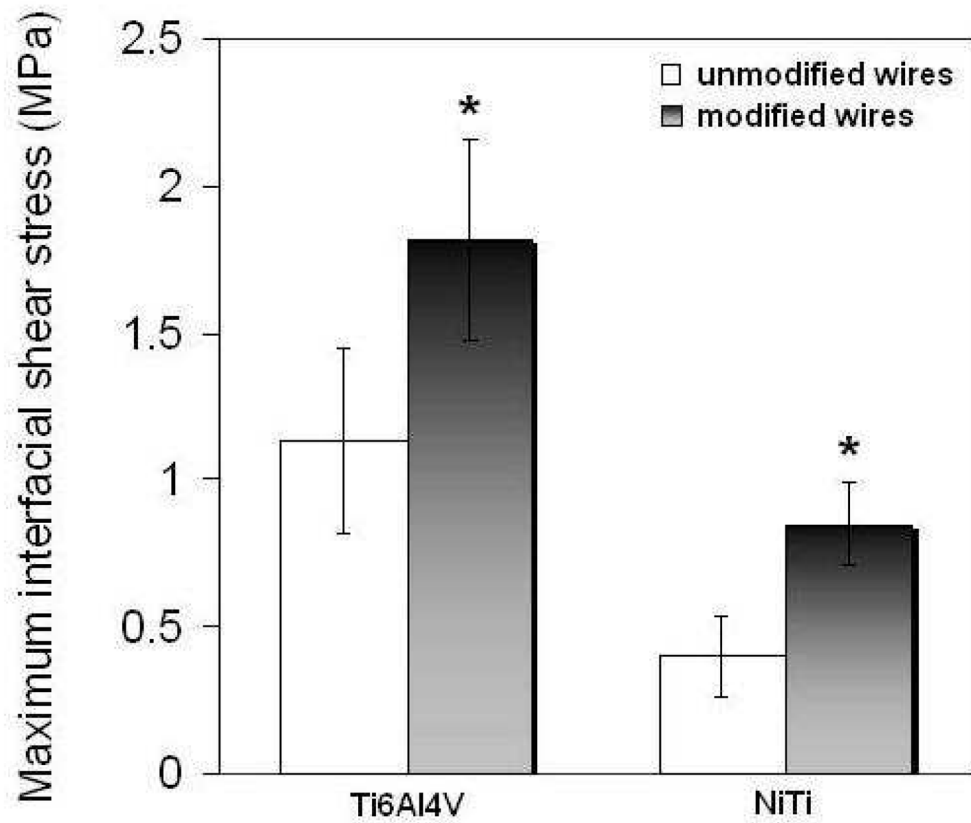
Figure 7.
Average maximum interfacial shear stress for modified and unmodified Ti-6Al-4V and NiTi wires pulled out from a PMMA matrix. Averages are calculated from between 9 and 16 specimens each of Ti-6Al-4V, modified Ti-6Al-4V, NiTi, and modified NiTi. Statistical significance (student's t test) is indicated by: *, $p < 0.05$ (compared to unmodified wires).